Design of broadband polarization converter for terahertz waves*

PAN Wu (潘武), **SHEN Da-jun** (沈大俊)**, **and YAN Yan-jun** (闫彦君)

College of Photoelectronic Engineering, Chongqing University of Posts and Telecommunications, Chongqing 400065, China

(Received 11 May 2018; Revised 11 June 2018)

A broadband reflective polarization converter is proposed. The unit cell of polarization converter is composed of a single-split resonant ring, a double-split resonant ring, a dielectric substrate and a metallic ground. The simulated results show that the polarization converter can convert *x*-polarized waves into *y*-polarized waves and obtain a broadband polarization conversion from 0.501 0 THz to 1.390 0 THz with the polarization conversion ratio (*PCR*) beyond 80% at normal incidence. Moreover, the surface current distributions are investigated to explain the polarization conversion mechanism. Finally, a good agreement is achieved between simulated and measured results. The polarization converter can be applied in terahertz imaging, communication and stealthy technology.

Document code: A **Article ID:** 1673-1905(2018)06-0434-4

DOI https://doi.org/10.1007/s11801-018-8072-3

Polarization is one of the fundamental characteristics of electromagnetic (EM) waves, which can be applied in circularly polarized antennas[1], radar technology[2] and wireless communication systems[3]. Thus, flexibly manipulating the polarization state of EM waves plays a significant role in electromagnetics. Traditional polarization converters are mainly designed using Faraday effect[4] and Brewster effect[5]. However, these conventional polarization conversion devices are limited in practical applications by low efficiency, narrow working bands and bulky volumes. In recent years, metamaterials have drawn increasing attention because of their unique EM properties, and also provide a new method to keep the high polarization conversion ratio (*PCR*) in a wide bandwidth.

In order to achieve high conversion efficiency and wide operating bandwidth, many polarization converters based on matematerials have been proposed in the past few years. Split ring resonators structure is commonly used to design polarization conversion devices. For example, Wen et al [6] proposed a high-efficiency polarization converter based on two single-split ring resonators, which can convert linearly polarized wave into its cross-polarization one, however, its operating bandwidth is narrow. To pursue the large polarization conversion bandwidth, Cheng et al[7] designed and demonstrated a wideband polarization converter on the basis of a double-split resonator and a metallic disk, but the *PCR* is low. To keep the high efficiency in a wide band, many structures based on split ring resonators have been proposed[8-10]. Xu et al[11] designed a polarization converter based on a double-split ring resonator with the polarization conversion efficiency of 75% from 0.67 THz to 2.41 THz. Fu et al[12] presented one broadband polarization converter based on resonant ring, which gave bandwidth from 0.59 THz to 1.24 THz with *PCR* above 80%. 2018, Li et al[13] designed a reflective polarization converter covering a frequency range of 0.4—1.04 THz with the *PCR* of 90%. Zhou et al[14] proposed a polarization converter using a L-shape structure, which provided *PCR* of 80% in the frequency range from 0.64 THz to 1.19 THz. From former studies, we can find that high conversion efficiency and wide working band can be achieved at the same time by changing the split width and ways.

Herein, we present a reflective polarization converter for terahertz waves of three layers composed of metasurface and a grounded metallic film separated by a dielectric substrate. The metasurface consists of a double-split resonant ring and a single-split resonant ring. The polarization converter can convert the *x*-polarized incident waves into *y*-polarized waves in the frequency range of 0.501 0—1.390 0 THz, with its efficiency more than 80%. Moreover, it can also convert the *y*-polarized incident waves into *x*-polarized waves with high efficiency.

Fig.1 presents the schematic diagram of the polarization converter. The unit cell is a classic three layer structure composed of metasurface and a grounded metallic film separated by a dielectric substrate. The metasurface

* This work has been supported by the New Direction Cultivation Project of Chongqing University of Posts and Telecommunications (No.A2014-116).

** E-mail: ks_shendajun@163.com

consists of a double-split resonant ring and a single-split resonant ring. The repeat period is $P=P_x=P_y$=80 μm, and other structural parameters are optimized as w=10 μm, r_1=35.5 μm, r_2=31.8 μm, r_3=18 μm, r_4=13 μm, α=90° and θ=105°. The proposed polarization converter was simulated by using the commercial software CST Microwave Studio 2017, where unit cell boundary condition was set in the x and y directions and open (add space) boundary condition was applied to the z-direction. In our simulation, the double-split resonant ring, the single-split resonant ring and metallic continuous film were made of lossy gold with a conductivity of $\sigma=4.56\times10^7$ S/m and a thickness of 0.3 μm. The dielectric material was selected as lossy quartz with relative permittivity of 3.75, loss tangent of 0.0004 and a thickness of d=37.0 μm.

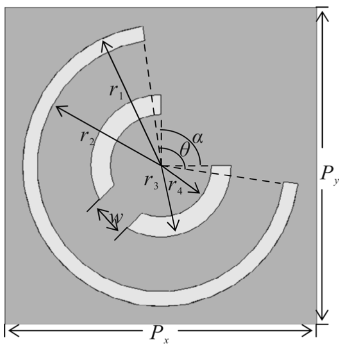

Fig.1 Schematic diagram of the proposed polarization converter

For better understanding the polarization conversion, the Jones matrix is introduced[14]. The reflection of linearly polarized incident fields through the polarization converter can be described as

$$\begin{pmatrix} E_x^{\rm r} \\ E_y^{\rm r} \end{pmatrix} = \begin{pmatrix} R_{xx} & R_{xy} \\ R_{yx} & R_{yy} \end{pmatrix} \begin{pmatrix} E_x^{\rm i} \\ E_y^{\rm i} \end{pmatrix}, \quad (1)$$

where $E_x^{\rm i}$ and $E_y^{\rm i}$ represent the incident electric fields at x- and y-component, $E_x^{\rm r}$ and $E_y^{\rm r}$ represent the reflected electric field at x- and y-component, $R_{mn}=r_{mn}{\rm e}^{{\rm i}\varphi_{mn}}$, r_{mn} represents the reflection coefficients for n-m polarization conversion, and φ_{mn} is the corresponding phase.

When the x-polarized wave is incident downward on the top surface of the polarization converter, the reflected electric field can be expressed as

$$\boldsymbol{E}^{\rm r} = E_x^{\rm r}\boldsymbol{x} + E_y^{\rm r}\boldsymbol{y} = r_{xx}{\rm e}^{{\rm i}\varphi_{xx}}E_x^{\rm i}\boldsymbol{x} + r_{yx}{\rm e}^{{\rm i}\varphi_{yx}}E_x^{\rm i}\boldsymbol{y}, \quad (2)$$

where $r_{xx} = \left|\boldsymbol{E}_{x\rm r}\right| / \left|\boldsymbol{E}_{x\rm i}\right|$ and $r_{yx} = \left|\boldsymbol{E}_{y\rm r}\right| / \left|\boldsymbol{E}_{x\rm i}\right|$ represent the co-polarization reflection coefficients and cross-polarization reflection coefficients, respectively. When r_{xx}=0, the reflected electric field can be calculated as

$$\boldsymbol{E}^{\rm r} = E_x^{\rm r}\boldsymbol{x} + E_y^{\rm r}\boldsymbol{y} = r_{xx}{\rm e}^{{\rm i}\varphi_{xx}}E_x^{\rm i}\boldsymbol{y}, \quad (3)$$

which means that the x-polarized waves are converted into y-polarized waves. In addition, the *PCR* is defined as $PCR = r_{yx}^2 / (r_{yx}^2 + r_{xx}^2)$.

Based on the above geometrical parameters, we simulate the polarization converter by using CST Microwave Studio. The reflection coefficients and *PCR* are presented in Figs.2 and 3, respectively.

From Fig.2, it can be seen that the simulated co-polarization reflection coefficients are less than 0.4, and the cross-polarization reflection coefficients are more than 0.8 from 0.501 THz to 1.390 THz. Additionally, we can see that the cross-polarization coefficients are 0.996, 1, 1 and 0.990 at four resonant frequencies of 0.526 4 THz, 0.760 0 THz, 1.214 4 THz and 1.537 6 THz, respectively. It means that nearly all energy of the incident x-polarized terahertz wave is converted to y-polarized wave at the four resonant frequencies. As shown in Fig.3, *PCR* is more than 80% in the frequency range of 0.501—1.390 THz, and the *PCR* nearly achieves 100% at the four resonance frequencies of 0.526 4 THz, 0.760 0 THz, 1.214 4 THz and 1.537 6 THz. It also confirms that the x-polarized wave is converted into y-polarized wave.

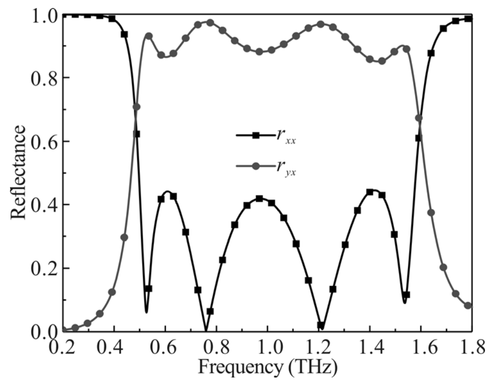

Fig.2 Reflection coefficients of the polarization converter at normal incidence

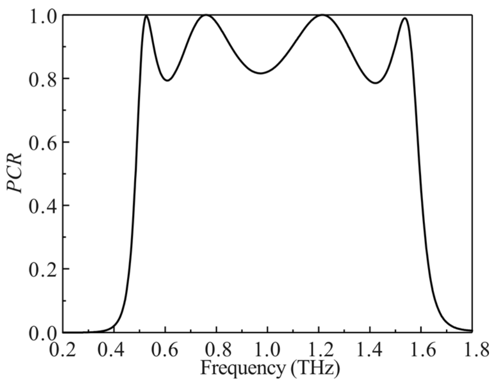

Fig.3 *PCR* of the proposed polarization converter

In order to interpret the physical mechanism of the linear polarization conversion, we study the surface current distributions at four resonant frequencies of 0.526 4 THz (f_1), 0.760 0 THz (f_2), 1.214 4 THz (f_3) and 1.537 6 THz (f_4). Fig.4 presents the current distributions on top layer and bottom layer, respectively. It can be seen from Fig.4, the surface currents are mainly induced on the outer single-split resonant ring. Meanwhile, the currents on the top layer at f_1 and f_2 are anti-parallel with the ones on the bottom layer, respectively. Therefore, resonances at f_1 and f_2 are caused by magnetic resonances. The parallel currents at f_3 and f_4 are obtained on the top layer and bottom layer, which means that the third resonance results from an electric resonance. In other words, the polarization conversion is due to the strong electromagnetic resonances in the polarization converter structure.

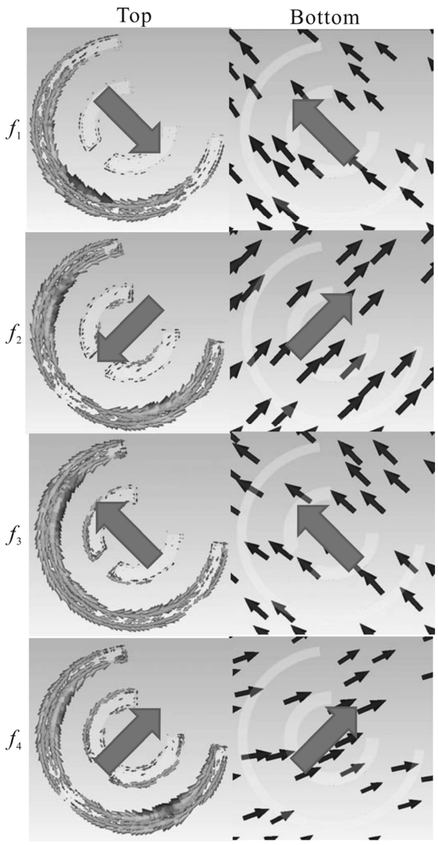

Fig.4 Surface current distributions on top layer and bottom layer at resonant frequencies

In order to experimentally show the polarization conversion performance of the proposed polarization converter, we fabricated the experimental sample with an area of 10 mm×10 mm as shown in Fig.5, containing 125×125 unit cells.

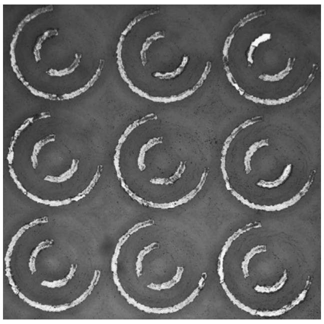

Fig.5 The prototype of the designed polarization converter

We use T-ray 500 to measure the co-polarization and cross-polarization reflection coefficients. The simulated and the measured results are shown in Fig.6. It can be clearly seen that the measured results of co-polarization reflection coefficients $r_{xx\text{-exp}}$ are roughly more than 0.4 from 0.508 5 to 1.451 6 and $r_{yx\text{-exp}}$ are higher than 0.8. Additionally, we can observe that the measured results are lower than simulated results, which is caused by the absorption of water vapor. In these four resonant frequencies, $r_{xx\text{-exp}}$ are nearly 0, which is the same with the simulated results.

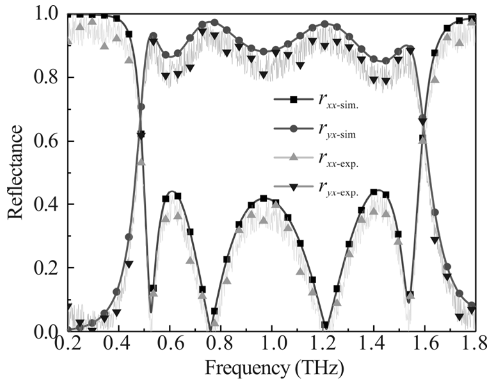

Fig.6 Reflection coefficients of simulated and measured results

In this paper, we design a broadband polarization converter. The proposed reflective polarization converter can convert the *x*-polarized wave into *y*-polarized wave in the frequency range from 0.508 5—1.451 6 THz and the *PCR* is greater than 80%. Furthermore, we interpret the physical mechanism of the linear polarization conversion by studying the surface current distributions. Finally, we fabricate and measure the polarization converter, and the simulated results are in agreement with measured results. The proposed polarization converter can also be used to convert *y*-polarized wave to *x*-polarized wave, and by changing the structural parameters, it can have many potential applications in microwave, terahertz and optical regimes.

References

[1] Li J, Zhang A, Joines W T and Liu QH, A miniaturized circularly polarized microstrip antenna with bandwidth enhancement, IEEE International Symposium on Antennas and Propagation, 41 (2016).

[2] Ryzhkov A V, Giangrande S E, Melnikov V M and Schuur T J, Journal of Atmospheric & Oceanic Technology **22**, 1138 (2004).

[3] Maltsev A, Perahia E, Maslennikov R, Sevastyanov A, Lomayev A and Khoryaev A, IEEE Antennas & Wireless Propagation Letters **9**, 413 (2010).

[4] Meissner T and Wentz F J, IEEE Transactions on Geoscience & Remote Sensing **44**, 506 (2006).

[5] Bao Q, Zhang H, Wang B, Ni Z, Lim, C, Wang Y, Tang D and Loh K, Nature Photonics **5**, 411 (2011).
[6] Zheng J and Wen X, Optics Express **22**, 28292 (2014).
[7] Cheng Y Z, Withayachumnankul W, Upadhyay A, Hiadland D, Nie Y, Gong R, Bhaskaran M, Sriram S and Abbott D Applied Physics Letters **105**, 26 (2014).
[8] Chen H Y, Wang J F, Ma H, Qu S B, Zhang J Q, Xu Z and Zhang A X, Chinese Physics B **24**, 253 (2015).
[9] Liu Y, Xia S, Shi H, Zhang A and Xu Z, Applied Physics B **122**, 178 (2016).
[10] Li S J, Xu L M, Cao X Y, Han J, Zhang Z, Liu X, Feng K and Zhang C, Radio-engineering **25**, 707 (2016).
[11] Xu K K, Xiao Z Y and Tang J Y, Plasmonics **12**, 1 (2016).
[12] Zhou L, Zhao G Z and Li Y H, Laser & Optoelectronics Progress **55**, 041602 (2018). (in Chinese)
[13] Li Y H, Zhou L and Zhao G Z, Chinese Journal of Laser **45**, 0314001 (2018). (in Chinese)
[14] Fu Y N, Zhang X Q, Zhao G Z, Li Y H and Yu J Y, Acta Physica Sinica **66**, 180701 (2017). (in Chinese)
[15] Chen H T, Taylor A J and Yu N, Reports on Progress in Physics Physical Society **79**, 076401 (2016).